A Combined Iterative and Boundary Element Approach for Solution of the Nonlinear Poisson-Boltzmann Equation

Y. N. Vorobjev,† J. A. Grant, and H. A. Scheraga*

Contribution from the Baker Laboratory of Chemistry, Cornell University, Ithaca, New York 14853-1301. *Received October 8, 1991*

Abstract: A general numerical method is presented to solve the nonlinear Poisson-Boltzmann (NLPB) equation for an arbitrarily-shaped solute. The essence of the method is the separation of the calculation of the solvent reaction potential from that of the potential due to the ion distribution. The solvent reaction potential is calculated by using an efficient boundary element method. The ion-induced potential is then calculated by means of an efficient volume integration using an iterative solution of the NLPB equation coupled to the fixed molecular and solvent electrostatic potential. At an ionic strength of ≤ 1 M the mobile ion distribution is determined primarily by the solute and the solvent reaction electrostatic potentials; as a consequence, rapid convergence of the iterative procedure is obtained. The accuracy of the results obtained by using the iterative boundary element (IBE) method is tested by comparison with analytical Tanford-Kirkwood results for a model spherical "protein" solute system. Results are also presented for the terminally blocked amino acid *N*-acetyl-alanyl-*N'*-methylamide (NANMA) and terminally blocked oligo-lysine peptides. It is found that the IBE method has some computational advantages with respect to the general finite-difference method in applications to large molecules.

Introduction

Electrostatic interactions are important factors in determining the native structures of both proteins and nucleic acids as well as their complexes with low-molecular-weight drugs.[1-3] The long-range nature of electrostatic interactions, even in aqueous solution, is one reason why their theoretical treatment is difficult. In order to circumvent the considerable and often prohibitive computational expense of microscopic (explicit) solvent models which, in principle, afford an exact treatment of electrostatic interactions in solution, there has been much renewed interest in the use of simpler continuum models.[1-9] In one class of continuum models,[5-9] the explicit structural features of the solvent are replaced by a linear high dielectric constant continuum surrounding the solute, which is modeled as a low dielectric constant charge-containing cavity. For ionic solutions, the ion distribution is modeled as a mean field, determined from statistical mechanics according to a Boltzmann distribution. The solute charge distribution and, at nonzero ionic strength, the mobile-ion distribution polarize the solvent, giving rise to a solvent reaction potential. The calculation of the polarization of the solvent is carried out by solving the Poisson equation or, when ionic-strength effects are to be included, by solving the more general Poisson-Boltzmann (PB) equation.

The interaction of the solvent reaction potential with the solute charge distribution determines the free energy of solvation of the system. Although very simple, such continuum models have been useful for making predictions concerning electrostatic effects in proteins,[10-12] which show reasonable agreement with experimental observations. A set of very elegant calculations has recently shown that continuum models reproduce solute-solvent free energies obtained by using a microscopic treatment of the solvent.[13] It is likely that the success of such continuum models is in part due to cancellation effects in the behavior of water at the molecular level.[14,15] The use of such continuum models is especially suitable for aqueous systems because of the unique behavior of the local dielectric constant in the region of the dielectric boundary. At the boundary, the dielectric constant varies very rapidly over a microscopic distance to the value of the dielectric constant for bulk water. This is consistent with the assumption in the continuum model that there are only two (discontinuous) dielectrics separated by a molecular interface. In addition, calculations of the potential of mean force between ions in aqueous solution using integral-equation theories[16] have shown that water completely screens vacuum Coulombic interactions within one hydration shell. Such behavior is well represented by simple continuum models.

Analytical solutions of the PB equation can be obtained for only a very few, simple cavity shapes. Hence, in order to study macromolecular systems in aqueous ionic solution using cavity-based continuum models, efficient methods for obtaining approximate numerical solutions to the PB equation have been developed, although some drawbacks remain with each method. There are broadly two different approaches in seeking approximate numerical solutions of the PB equation. One such approach is the finite-difference (FD) method, first used to study biomacromolecular systems by Warwicker and Watson,[5] with several very important algorithmic advances being added later by Gilson et al.[17] and Nicholls and Honig.[18] The finite-difference method is very general and has been used to obtain solutions of the full non-linear Poisson-Boltzmann (NLPB) equation.[19] In this method, the solute and solvent are mapped onto a cubic lattice. Each of the small cubes defining the lattice is assigned an appropriate value of the charge density, dielectric constant, and ionic-strength parameters that appear in the PB equation. The method of finite-differences is then used to obtain the electrostatic potential over the entire grid iteratively. This technique involves N^3 variables (the total number of lattice sites), where N is the

† On leave from Novosibirsk Institute of Bio-organic Chemistry, Novosibirsk, 630090, USSR.

* Author to whom correspondence and reprint requests should be addressed.

(1) Harvey, S. C. *Proteins: Struct., Funct. Genet.* **1989**, *5*, 78-92.
(2) Davis, M. E.; McCammon, J. A. *Chem. Rev.* **1990**, *90*, 509-521.
(3) Sharp, K. A.; Honig, B. *Annu. Rev. Biophys. Biophys. Chem.* **1990**, *19*, 301-332.
(4) Scheraga, H. A.; Katchalsky, A.; Alterman, Z. *J. Am. Chem. Soc.* **1969**, *91*, 7242-7249.
(5) Warwicker, J.; Watson, H. C. *J. Mol. Biol.* **1982**, *157*, 671-679.
(6) Gilson, M. K.; Rashin, A.; Fine, R.; Honig, B. *J. Mol. Biol.* **1985**, *184*, 503-516.
(7) Zauhar, R. J.; Morgan, R. S. *J. Mol. Biol.* **1985**, *186*, 815-820.
(8) Klapper, I.; Hagstrom, R.; Fine, R.; Sharp, K. A.; Honig, B. *Proteins: Struct., Funct. Genet.* **1986**, *1*, 47-59.
(9) Rashin, A.; Namboodiri, K. *J. Phys. Chem.* **1987**, *91*, 6003-6012.
(10) Matthew, J. B. *Annu. Rev. Biophys. Biophys. Chem.* **1985**, *14*, 387-417.
(11) Gilson, M. K.; Honig, B. H. *Nature* **1987**, *330*, 84-86.
(12) Sternberg, M. J. E.; Hayes, F. R. F.; Russell, A. J.; Thomas, P. G.; Fersht, A. R. *Nature* **1987**, *330*, 86-88.
(13) Jean-Charles, A.; Nicholls, A.; Sharp, K. A.; Honig, B.; Tempczyk, A.; Hendrickson, T. F.; Still, W. C. *J. Am. Chem. Soc.* **1991**, *113*, 1454-1455.
(14) Jayaram, B.; Fine, R.; Sharp, K. A.; Honig, B. *J. Phys. Chem.* **1989**, *93*, 4320-4327.
(15) Roux, B.; Yu, H. A.; Karplus, M. *J. Phys. Chem.* **1990**, *94*, 4683-4688.
(16) Patey, G. N.; Carnie, S. L. *J. Chem. Phys.* **1983**, *78*, 5183-5190.
(17) Gilson, M. K.; Sharp, K. A.; Honig, B. H. *J. Comput. Chem.* **1987**, *9*, 327-335.
(18) Nicholls, A.; Honig, B. *J. Comput. Chem.* **1991**, *12*, 435-445.
(19) Jayaram, B.; Sharp, K. A.; Honig, B. *Biopolymers* **1989**, *28*, 975-993.

0002-7863/92/1514-3189$03.00/0

number of points per edge of the lattice.

There are some difficulties encountered when using finite-difference techniques. One concerns the necessary choice of boundary conditions. These can be obtained at sufficiently large distance with respect to the dielectric boundary from either Coulomb's law or Debye–Hückel theory. To achieve a high degree of accuracy, it is necessary to consider the continuum solvent that is far from the solute; this entails increasing the lattice size (relative to the molecule) and hence the expense of the calculation. A second problem associated with the finite-difference technique arises because of the necessity to map the molecular charge distribution onto lattice points. The resulting error arising from this disturbance of the optimal charge distribution is a function of the lattice spacing (although it is in general small); however, when the molecular charge distribution is approximated by a set of distributed multipoles, it is likely that mapping onto the lattice would have to be achieved by use of a limiting monopole distribution. Faerman and Price[20] have recently demonstrated the utility of using such a distributed multipole description to obtain very accurate descriptions of the electrostatic field/potential at the molecular surface, for peptide molecules, a prerequisite for the success of electrostatic continuum solvent models.

An alternative approach for obtaining solutions of the Poisson equation is the boundary element method, first developed for macromolecules by Zauhar and Morgan,[7] with different algorithmic improvements proposed by Rashin and Namboodiri[9] and Zauhar and Morgan.[21,22]

The key feature of the boundary element method is the reduction of the problem to the solution of an integral equation over a two-dimensional surface. The polarization of the solvent by the solute induces a field throughout the volume of the surrounding dielectric medium. Calculation of the polarization field is equivalent to the calculation of induced polarization charge density at the dielectric boundary.[7,23]

The boundary element method is a function of S independent variables, where S is the number of elements covering the two-dimensional surface, which serves as the dielectric interface. There is no requirement to displace atomic charge distributions when using this method, and in general the method allows for a more accurate description of the molecular surface than the finite-difference method. The boundary element method has thus far been used to calculate the total electrostatic potential and the associated electrostatic component of the free energy of solvation.[7,9] Rashin[24] has described a combined iterative boundary element method to obtain solutions of the general PB equation, but has not presented details for carrying out accurate volume integrations, or about the convergence properties of the scheme.

The inclusion of ionic-strength effects in continuum models is often achieved by using a linearized version of the Poisson–Boltzmann equation.[1,17,25,26] Unlike the full nonlinear version, the linear Poisson–Boltzmann (LPB) equation is formally correct in the limit of low ionic strength and can be derived within a statistical mechanical framework from a partition function.[26] However, use of the LPB equation is unlikely to be suitable for all investigations concerning macromolecular structure. This is because, even at low ionic strength, the main condition for linearization, i.e., $q_i\Phi(r)/kT \ll 1$ [where $\Phi(r)$ is the electrostatic potential, q_i is the ion charge, T is temperature, and k is the Boltzmann constant], appears to break down at room temperature in aqueous solution if the distance between an ion and an exposed polar atom is smaller than 5 Å, according to our calculations. The ion charge density predicted by the LPB equation is generally too low and leads to incorrect estimations of ion screening between charged atoms. A detailed discussion concerning the validity of the NLPB equation, as well as derivations of various forms of the associated total electrostatic energy, has been given recently by Sharp and Honig.[27]

The purpose of the present paper is to develop a procedure to obtain solutions to the NLPB equation within the framework of the previously described boundary element method. The underlying physical basis of our method is our observation that, at relatively low ionic strength ($\leq$1 M), the distribution of mobile ions around the solute molecule is determined primarily by the potential due to the solute charge distribution and the reaction solvent potential (viz. the potential due to the surface charges obtained in the boundary element method). This makes possible the calculation of the mobile ion distribution around the molecule in the following way. First, the polarization of the solvent by the solute charge distribution is calculated by using a boundary element method. We then take into account the remaining terms that determine the ion distribution, namely, direct ion–ion interactions and van der Waals interactions with the solute (in addition to the solute and reaction potentials). Because the ion–solvent polarization depends on the mobile ion density, which itself depends on the ion–solvent polarization, the distribution of mobile ions must be obtained *iteratively*. Thus, a self-consistent mean field is obtained to describe the influence of mobile ions within the continuum solvent framework. This is a qualitative description of the iterative boundary element (IBE) method, which makes use of the exact charge density distribution inside the solute molecule to obtain a solution of the NLPB equation. It is possible to apply the IBE method to a protein, and we shall demonstrate that there are some advantages in this technique compared to the finite-difference method.

Details of the IBE Method

We consider a solvated molecule to be comprised of a cavity of low dielectric constant D_i embedded in a continuum solvent medium of high dielectric constant D_o. The solute is separated from the solvent by a boundary, which is defined to be the smooth surface traced by the inward-facing part of a probe (with the radius of a water molecule) as it rolls over the solute molecule.[28,29] An analytical description of this surface has been described by Connolly.[30] This boundary confines the solute molecular charge distribution, which is typically represented as a set of fixed charges $\{q_k\}$ located at atomic centers $\{\mathbf{r}_k\}$. Mobile ions are not represented explicitly, but appear as a statistically determined mean field. By taking advantage of the law of superposition, the total electrostatic potential Φ_{total} can be written as:

$$\Phi_{total}(\mathbf{r}) = \Phi_{mol}(\mathbf{r}) + \Phi_r(\mathbf{r}) + \Phi_{ion}(\mathbf{r}) \quad (1)$$

where Φ_{mol} is the potential due to the solute charge distribution, Φ_r is the reaction potential, arising from the linear response of the solvent dielectric medium to the solute charge distribution, and Φ_{ion} is the potential due to the mean field of the ion distribution. The sum of the potentials, $\Phi_{mol} + \Phi_r$, satisfy the Poisson equation, namely:

$$\nabla\cdot D(\mathbf{r})\nabla[\Phi_{mol}(\mathbf{r}) + \Phi_r(\mathbf{r})] + 4\pi\sum_k q_k\delta(\mathbf{r} - \mathbf{r}_k) = 0 \quad (2)$$

where $\mathbf{r}_k$ is the position of a set of fixed charges within the solute cavity, and $D(\mathbf{r})$ is the dielectric constant at point $\mathbf{r}$. It is possible to obtain solutions to eq 2 by any implementation of the boundary element method.[7,9,21,22] The molecular potential Φ_{mol} is given straightforwardly by:

$$\Phi_{mol}(\mathbf{r}) = \frac{1}{D_i}\sum_k \frac{q_k\delta(\mathbf{r} - \mathbf{r}_k)}{|\mathbf{r} - \mathbf{r}_k|} \quad (3)$$

and the reaction potential Φ_r is obtained from the surface integral

(20) Faerman, C. H.; Price, S. L. *J. Am. Chem. Soc.* **1990**, *112*, 4915–4926.
(21) Zauhar, R. J.; Morgan, R. S. *J. Comput. Chem.* **1988**, *9*, 171–187.
(22) Zauhar, R. J.; Morgan, R. S. *J. Comput. Chem.* **1990**, *11*, 603–622.
(23) Reitz, J. R.; Milford, F. J. *Foundations of Electromagnetic Theory*; Addison-Wesley: Reading MA, 1968; p 70.
(24) Rashin, A. A. *J. Phys. Chem.* **1990**, *94*, 1725–1733.
(25) Bashford, D.; Karplus, M. *Biochemistry* **1990**, *29*, 10219–10225.
(26) McQuarrie, D. A. *Statistical Mechanics*; Harper and Row: New York, 1976; Chapter 15.
(27) Sharp, K. A.; Honig, B. *J. Phys. Chem.* **1990**, *94*, 7684–7692.
(28) Richards, F. M. *Annu. Rev. Biophys. Bioeng.* **1977**, *6*, 151–176.
(29) Connolly, M. L. *Science* **1983**, *221*, 709–713.
(30) Connolly, M. L. *J. Appl. Crystallogr.* **1983**, *16*, 548–558.

$$\Phi_r(\mathbf{r}) = \int_S \frac{\sigma(\mathbf{s})\,d\mathbf{s}}{|\mathbf{r}-\mathbf{s}|} \tag{4}$$

where the surface charge density $\sigma(\mathbf{s})$ at $\mathbf{s}$ is determined by the integral equation[9]

$$\sigma(\mathbf{t}) = f\int_S \frac{\sigma(\mathbf{s})(\mathbf{t}-\mathbf{s})\mathbf{n}(\mathbf{t})\,d\mathbf{s}}{|\mathbf{t}-\mathbf{s}|^3} + \frac{f}{D_i}\sum_k \frac{q_k(\mathbf{t}-\mathbf{r}_k)\mathbf{n}(\mathbf{t})}{|\mathbf{t}-\mathbf{r}_k|^3} \tag{5}$$

where the constant f is

$$f = \frac{1}{2\pi}\frac{D_i - D_o}{D_i + D_o} \tag{6}$$

and $\mathbf{n}(\mathbf{t})$ is the vector normal to the surface at the point $\mathbf{t}$. The last term in eq 5 is the normal component of the electrostatic field due to the solute charge distribution. In the boundary element method, the integral appearing in the first term of eq 5 is replaced by a discrete sum over a finite number of boundary elements which tesselate the molecular surface. Although eqs 3 and 5 are written in terms of a set of distributed monopoles, use of alternative representations of the molecular charge density, such as distributed multipoles or that calculated from an ab initio wave function,[31] is straightforward.

The potential due to the mean field ion distribution is given by the NLPB equation; thus

$$\nabla\cdot D(\mathbf{r})\nabla\Phi_{ion}(\mathbf{r}) + 4\pi\rho_{ion}(\mathbf{r}) = 0 \tag{7}$$

$\rho_{ion}(\mathbf{r})$ is the total ionic charge density given by:

$$\rho_{ion}(\mathbf{r}) = \sum_l \rho_l^0 Z_l \exp\{-[Z_l\Phi_{mol}(\mathbf{r}) + \Phi_r(\mathbf{r}) + \Phi_{ion}(\mathbf{r})] + U^l_{nb}(\mathbf{r})/kT\} \tag{8}$$

The index l in eq 8 runs over the different ion species in solution, and Z_l and ρ_l^0 are the ion charge and bulk density, respectively, of the lth ionic species. $U^l_{nb}(\mathbf{r})$ is the potential energy of the nonbonded interaction of ion type l with the solute. This nonbonded term serves in part to account for the finite size of the ions and is usually taken to be independent of ion type (see, for example, refs 25 and 32). There is no difficulty, however, in our implementation in assigning different nonbonded parameters to model different ion species.

The potential due to the ion distribution $\Phi_{ion}(\mathbf{r})$ appearing in eq 8 can be decomposed into a sum of a direct term, plus a reaction term arising from contributions due to solvent response, so that

$$\Phi_{ion}(\mathbf{r}) = \Phi_{id}(\mathbf{r}) + \Phi_{ir}(\mathbf{r}) \tag{9}$$

where the direct term is given by:

$$\Phi_{id}(\mathbf{r}) = \frac{1}{D_o}\int_{V_{out}} \frac{\rho_i(\mathbf{t})\,d\mathbf{t}}{|\mathbf{r}-\mathbf{t}|} \tag{10}$$

where the limit of integration V_{out} is used to indicate that numerically we carry out the integration over a finite volume. The reaction potential $\Phi_{ir}(\mathbf{r})$ can be expressed in terms of a surface charge density $\sigma_{ir}(\mathbf{s})$ induced on the molecular surface, such that

$$\Phi_{ir}(\mathbf{r}) = \int_S \frac{\sigma_{ir}(\mathbf{s})\,d\mathbf{s}}{|\mathbf{r}-\mathbf{s}|} \tag{11}$$

The surface charge density $\sigma_{ir}(\mathbf{s})$ can be obtained from an integral equation similar to eq 5, viz.:

$$\sigma_{ir}(\mathbf{t}) = f\int_S \frac{\sigma_{ir}(\mathbf{s})(\mathbf{t}-\mathbf{s})\mathbf{n}(\mathbf{t})\,d\mathbf{s}}{|\mathbf{t}-\mathbf{s}|^3} + \frac{f}{D_o}\int_V \frac{\rho_{ion}(\mathbf{p})(\mathbf{t}-\mathbf{p})\mathbf{n}(\mathbf{t})\,d\mathbf{p}}{|\mathbf{t}-\mathbf{p}|^3} \tag{12}$$

where $\mathbf{s}$ and $\mathbf{p}$ are integration variables. The last term in eq 12 is the normal component of the field due to the mobile ions at a point $\mathbf{t}$ on the molecular surface. Expressions for the surface charge densities in both eqs 5 and 12 can be expressed as a set of linear equations in matrix form;[31] thus:

$$\mathbf{K}\sigma = \mathbf{b} \tag{13}$$

The matrix $\mathbf{K}$ is purely a function of the geometric properties of the boundary elements that cover the molecular surface, and needs to be computed only once. A complete definition of the matrix elements of $\mathbf{K}$, as it is used in this work, is given in ref 31. The right-hand side of eq 13 is a function of the normal component of the field, due to either the solute charge distribution when solving eq 5, or the mobile ions when solving eq 12. Since Φ_{ion} in eq 7 is coupled to $\rho_{ion}(\mathbf{r})$ through eq 8, eqs 8 through 12 must be solved iteratively, for example, by setting $\Phi_{ion}(\mathbf{r})$ initially to zero.

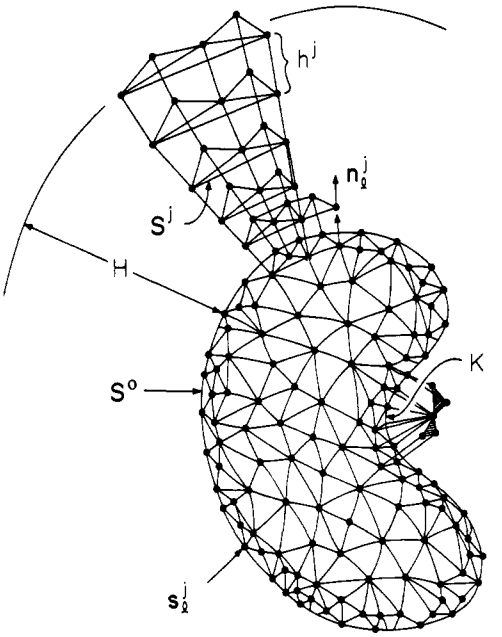

Figure 1. Schematic illustration of the boundary element based grid (BEBG). The dots represent the center of the boundary elements. S^0 denotes the molecular surface which serves as the dielectric boundary, S^j denotes an expanded surface, and $\mathbf{n}^j_l$ is the vector normal to the lth boundary element, s^j_l, on the surface S^j. h_j is the thickness of the jth shell, and H is the total thickness of the ion atmosphere. The point K is on a concave region of the molecular surface and illustrates the use of pyramidal concave elements. It is important to observe that we represent the surface elements as triangles for pictorial convenience only. The actual surface elements comprise concave spherical triangles, rectangular saddles, and arbitrary convex polygons.

Numerical Algorithm for the IBE Method

There are two principal components of the IBE method. First, it is necessary to obtain the solvent reaction potential using a boundary element technique. Our implementation of this method[31,33] is very similar to the method of Rashin and Namboodiri,[9] in which two sets of boundary elements at different densities cover the surface. The use of two different densities for the boundary elements improves the description of the surface charge density with respect to curvature of the surface. Unlike Rashin and Namboodiri, we employ a full analytical description of the molecular surface as given by Connolly,[30] which also serves to improve the accuracy of the boundary element description.[33]

Once the solvent reaction potential has been obtained, the second step involves the calculation of the total electrostatic potential from the iterative solution of the NLPB as described in the previous section (eqs 8 through 12). This requires an integration over the volume that is external to the solute cavity to calculate $\Phi_{id}(\mathbf{r})$ and $\Phi_{ir}(\mathbf{r})$ (eqs 10 and 11, respectively). To carry

(31) Grant, J. A.; Williams, R. L.; Scheraga, H. A. *Biopolymers* **1990**, *30*, 929–949.
(32) Gilson, M. K.; Honig, B. H. *Proteins: Struct., Funct. Genet.* **1988**, *3*, 32–52.
(33) Grant, J. A.; Williams, R. L.; Scheraga, H. A. In preparation.

out such an integration, we take advantage of the fact that we have a geometrical description of the molecular surface partitioned into boundary elements. This enables us to construct a three-dimensional space grid of nonregular volume elements v_l external to the molecular cavity. We proceed as follows. First we calculate a family of molecular surfaces $\{\mathbf{S}^j\}$ where $j = 0, 1, ..., n_{sh}$, where n_{sh} is the total number of surfaces external to the dielectric boundary (see Figure 1). The surface $\mathbf{S}^0$ is the molecular surface which serves as the dielectric interface in the calculation of the solvent reaction potential, and is constructed from the smooth surface traced by the inward-facing part of the probe as it rolls over the interlocking atom-centered spheres of atomic radii R^0. This surface is covered with a set of boundary elements defined by the position vector $\mathbf{s}_l^j$, the area Δs_l^j, and the vector normal to the surface $\mathbf{n}_l^j$. Surface $\mathbf{S}^{j+1}$ and associated boundary elements are calculated in the same way using a set of atomic radii R^{j+1} obtained by incrementing the atomic radii corresponding to the surface $\mathbf{S}^j$ by an amount h^j. The density of boundary elements covering the family of molecular surfaces is kept constant; therefore, prior to the construction of the volume elements, there are always more boundary elements on the surface $\mathbf{S}^{j+1}$ than on the surface $\mathbf{S}^j$. The last surface $\mathbf{S}^j$ ($j = n_{sh}$) encloses the (finite) volume of the integration, and hence the total thickness of the ion atmosphere H will be taken as the sum of all h^j. It is not necessary for the increment h^j to be constant, with respect to consecutive surfaces. In general, we choose larger values of h^j as j increases. We shall return to this point later.

It is now possible to construct a set of volume elements v_l connecting the boundary elements of two consecutive surfaces. Obviously for convex regions the shapes of the volume elements are prisms. For concave regions, some of the volume elements will be pyramids; this is illustrated in Figure 1 at point K. To determine the position $\mathbf{r}_l^j$ and the volume v_l of the volume elements, we connect each surface element $\mathbf{s}_{l'}^{j+1}$ of surface $\mathbf{S}^{j+1}$ with the closest surface element $\mathbf{s}_l^j$ of the surface $\mathbf{S}^j$. Each pair of surface elements $\mathbf{s}_{l'}^{j+1}$ and $\mathbf{s}_l^j$ defines the top and bottom faces of a prismatic volume element, whose position and volume are given by

$$\mathbf{r}_l^j = \frac{(\mathbf{s}_{l'}^{j+1} + \mathbf{s}_l^j)}{2} \tag{14}$$

$$v_l^j = \frac{(\Delta s_{l'}^{j+1}\mathbf{n}_{l'}^{j+1} + \Delta s_l^j\mathbf{n}_l^j)}{2}(\mathbf{s}_{l'}^{j+1} - \mathbf{s}_l^j) \tag{15}$$

There are two special cases that need to be considered when constructing the general volume elements. The first case occurs when two or more elements on the surface $\mathbf{S}^{j+1}$ are connected to the *same* element on the surface $\mathbf{S}^j$; then those on the upper surface are coalesced to make a single boundary element whose area is the sum of the areas of the individual elements, and whose location is the mean of the positions of the individual elements. This modified boundary element replaces the previous ones for the rest of the calculations. Finally, we search for elements $\mathbf{s}_{l(cv)}^j$ which belong to concave regions of surface $\mathbf{S}^j$ and have no connection with any surface element of the surface $\mathbf{S}^{j+1}$. These surface elements $\mathbf{s}_{l(cv)}^j$ form the bottom face of pyramidal volume elements. The position of the vertex of each pyramid is the closest point $\mathbf{s}_{l'(cv)}^{j+1}$ on the surface $\mathbf{S}^{j+1}$. The position and volume of these pyramidal elements are given by

$$\mathbf{r}_{l(cv)}^j = (1/3)(\mathbf{s}_{l'(cv)}^{j+1} + \mathbf{s}_{l(cv)}^j) \tag{16}$$

$$v_{l(cv)}^j = (1/3)\Delta s_{l(cv)}^j\mathbf{n}_{l(cv)}^j\cdot(\mathbf{s}_{l'(cv)}^{j+1} - \mathbf{s}_{l(cv)}^j) \tag{17}$$

By calculating the positions and the volumes of the volume elements as described, for all pairs of consecutive shells up to $\mathbf{S}^j$, $j = n_{sh}$, we have a boundary-element-based grid (BEBG) which describes the volume external to the molecular cavity. We also find it advantageous to choose the increment h^j between consecutive shells to be larger as we move away from the dielectric boundary. This is reasonable because the ion distribution becomes increasingly uniform in regions distant from the molecular surface. We find that the BEBG accurately describes the volume close to the molecular surface, while reducing considerably the number of volume elements required compared to a regular rectangular grid. The following expression is used to carry out numerical integrations for functions $f(\mathbf{r})$ over the volume V_{out} that is external to the molecular cavity:

$$\int_{V_{out}} f(\mathbf{r})\,d\mathbf{v} = \sum_{j=0}^{n_{sh}-1}\sum_{l=1}^{S^j} f(\mathbf{r}_l^j)v_l^j \tag{18}$$

where $\mathbf{r}_l^j$, v_l^j are the position and the volume of the lth volume element, and S^j is the number of boundary elements on the surface $\mathbf{S}^j$.

In order to estimate the total number of operations required by the IBE method, as compared to the finite-difference method, we assume for the finite-difference method a lattice dimension N, and lattice-box occupancy of 50%; then an approximate relation for the number of boundary elements S in terms of N is:

$$S \approx 6(N/2)^2 \approx N^2 \tag{19}$$

The total number of grid points N_{BEBG} is:

$$N_{BEBG} = n_{sh}N^2 \tag{20}$$

Assuming n_{iter} iterations to obtain convergence, we have the following estimate for the number of operations required by the IBE method (n_{IBE}):

$$n_{IBE} \approx (N^2)^3 + N^2(n_{sh}N^2)n_{iter} + (n_{sh}N^2)^2n_{iter} \tag{21}$$

The first term in eq 21 describes the number of operations required to obtain the solvent reaction potential from eq 5. This essentially involves the once-only calculation of the matrix $\mathbf{K}^{-1}$ in eq 13, which can also be used later to obtain $\Phi_{ir}(\mathbf{r})$. Matrix inversion is an n^3 process, where n is the order of the matrix[34] (calculation of the surface area, normal, and coordinates of the boundary elements are trivial in comparison). The second and third terms in eq 21 are estimations of the number of operations to compute $\Phi_{ir}(\mathbf{r})$ and $\Phi_{id}(\mathbf{r})$, respectively. The most time-consuming part of the iterative component of the IBE method is found to be the recalculation of the direct ion potential $\Phi_{id}(\mathbf{r})$ at each point on the grid used in the numerical integration procedure.

To improve the convergence of the iterative solution of the NLPB equation, we use a simple "damping" procedure to construct the ionic density; thus:

$$\rho^{(k+1)}(\mathbf{r}) = \alpha\rho^{(k)}(\mathbf{r}) + (1 - \alpha)\rho^{(k-1)}(\mathbf{r}) \tag{22}$$

where α is an adjustable parameter. Similar methods are used to obtain iterative solutions for integral equations in liquid theory[35] and the Hartree–Fock equations.[36] We typically use a value of α between 0.1 and 0.25, and obtain convergence in the ion density after approximately 10 iterations or less.

To obtain converged solutions, we also make use of the fact that the ion distribution must neutralize each permanent multipole moment of the solute charge distribution. Thus, we have a set of integral conditions which the mobile ion distribution must obey. For example, for the total charge (monopole) of the solute (Q_m) we have:

$$\left|\int \rho_i(\mathbf{r})\,d\mathbf{v}\right| = |Q_m| \tag{23}$$

A similar condition can be written for any multipole moment of the solute charge distribution; for the solute dipole moment (μ_m), we have:

$$\left(\int \rho_i(\mathbf{r})\mathbf{r}\,d\mathbf{v} + \mu_m\right)\cdot\mu_m = 0 \tag{24}$$

We make use of these two conditions in the following way. At the beginning of the iterative calculations, the outer limit of the

(34) Press, W. H.; Flannery, B. P.; Teukolsky, S. A.; Vetterling, W. T. *Numerical Recipes. The Art of Scientific Computing*; Cambridge University Press, London, 1987.
(35) Hirata, F.; Rossky, P. J. *J. Chem. Phys.* **1981**, *74*, 5324–5326.
(36) Guest, M. F.; Saunders, V. *Mol. Phys.* **1974**, *28*, 819–828.

Table I. Comparison of IBE and Tanford–Kirkwood Results[a] for Solution of the Linear Poisson–Boltzmann Equation at 300 K, for a Model Spherical System in a 1:1 Salt at 0.5 M

S[b]	h', Å[c]	H, Å[d]	$\Phi_r(1)$[e]	$\Phi_r(2)$[f]	$\Phi_{ion}(1)$[e]	$\Phi_{ion}(2)$[f]	$\Delta(10)$[g]
123	0.50	10.0	118.685	19.063	0.763	0.182	0.01
188	0.50	10.0	118.916	19.035	0.773	0.226	0.007
351	0.50	10.0	117.956	18.956	0.628	0.303	0.056
188	0.75	15.0	118.916	19.035	0.650	0.244	0.110
188	0.30	20.0	118.916	19.035	0.742	0.218	0.016
analytical TK result			117.326	19.102	0.794	0.166	

[a] All potentials given in units of kcal mol^{-1}. [b] Number of surface boundary elements, for low-density surface coverage. [c] Uniform thickness of each shell. [d] Cutoff distance (outer boundary for the volume integration). [e] Potential at point (1) evaluated at (8.5, 0, 0). [f] Potential at point (2) evaluated at (−8.5, 0, 0). [g] Value of the integral in eq 25 after 10 steps.

volume integrations comprises only a few of the total number of spherical shells. The ion density is calculated (iteratively) until it satisfies the conditions in eqs 23 and 24 to a certain tolerance (typically a 10% error in each multipole moment). At this point a few more of the spherical shells are admitted into the volume integrations, and the iterative procedure is continued, until again the ion density satisfies the conditions of eqs 23 and 24 to the specified tolerance. This procedure is continued repeatedly until the outer shell of the volume integration is admitted. We find that performance of the integration in this manner prevents spatial oscillation in the mobile ion density. It should be noted that, although statistical mechanical electrolyte theories do predict actual spatial oscillations in the ion atmosphere,[37,38] these oscillations occur only at concentrations greater than 1 M, which is beyond the limit of general interest for the physical properties of protein solutions.

We define the convergence of the procedure to be attained when the following condition is satisfied for a normalized ion density:

$$\frac{1}{C}\int_{V_{out}} |\rho^k - \rho^{k-1}|\, d\mathbf{v} \leq \text{tol} \qquad (25)$$

where C is the molar concentration of the ions in the solution and tol is a predefined tolerance, typically chosen such that changes in the density between iterations is less than 1%.

At the end of the iterative procedure, errors introduced by carrying out numerical integrations over a finite volume mean that the exact conditions specified by eqs 23 and 24 are not fulfilled, and a residual charge associated with the average mobile ion charge density exists. This charge ΔQ_i is given by:

$$\Delta Q_i = -Q_m - \int_{V_{out}} \rho_{ion}(\mathbf{r})\, d\mathbf{v} \qquad (26)$$

where Q_m is the total solute charge. This residual charge is usually less than 10% of the solute charge. We introduce a correction to the total electrostatic potential by distributing a uniform potential inside the pseudosphere of radius R_{ps}, where R_{ps} is the average radius of the outer shell used in the numerical integration. This correction Φ_{ex} due to the excess charge, to be added to the total potential, is given by:

$$\Phi_{ex} = \Delta Q_i \kappa/(1 + R_{ps}\kappa) \qquad (27)$$

where κ is the Debye constant.

Test Results

To demonstrate the utility of the IBE method, we present results for a model spherical system and for the terminally blocked amino acid *N*-acetyl-alanyl-*N'*-methylamide (NANMA) and terminally blocked oligo-lysine peptides.

Model Spherical System. We consider first a calculation of the total electrostatic potential, in which the solute cavity is modelled as a sphere. We choose the radius of the sphere to be 10 Å, which crudely approximates the dimensions of a moderate-molecular-weight globular protein, and place a single positive charge inside the cavity at a distance d from the center of the sphere. For such a system, the well-known approach of Tanford and Kirkwood (TK) can be used to obtain analytical solutions for the LPB equation.[39–41] We therefore present in Table I results obtained by using the IBE method to solve the LPB equation and compare them to the analytical TK results. The calculations were carried out with a unit charge located at (8.5, 0, 0 Å), for a 1:1 salt at a concentration of 0.5 M and at a temperature of 300 K. This distance was chosen to be representative of the distance that an atomic charge can approach the dielectric boundary, given typical values of van der Waals radii. The internal dielectric constant D_i is chosen to be 1.00, and the outer dielectric constant D_o is 80.0. The reaction solvent potential Φ_r and the ion potential Φ_{ion} are calculated at both (±8.5, 0, 0 Å).

Table II. IBE Results[a] for Solution of the Nonlinear Poisson–Boltzmann Equation at 300 K, for a Model Spherical System in a 1:1 Salt at 0.5 M, h' = 0.5 Å, H = 10.0 Å, S = 188 (Tanford–Kirkwood Results for the Linear Poisson–Boltzmann Equation Are Given for Reference)

d, Å[b]	$\Phi^{IBE}(1)$[c]	$\Phi^{TK}(1)$[c]	$\Phi^{IBE}(2)$[d]	$\Phi^{TK}(2)$[d]	$\Phi e/kT$
0.0	32.774	32.774			≤0.5
	(0.286)	(0.298)			
5.0	43.526	43.623	26.071	26.258	≈1.0
	(0.472)	(0.386)	(0.363)	(0.238)	
7.5	74.456	74.573	20.771	21.040	>1.0
	(0.799)	(0.590)	(0.342)	(0.186)	
8.5	118.916	117.326	19.035	19.102	>1.0
	(1.144)	(0.794)	(0.202)	(0.166)	

[a] All potentials given in units of kcal mol^{-1}. Values are for Φ_r (values for Φ_{ion} are given in parentheses). [b] Position of unit charge placed along the radius of the sphere. [c] Potential at point (1) evaluated at (d, 0, 0). [d] Potential at point (2) evaluated at (−d, 0, 0).

Table I also illustrates the variation in the calculated potentials as a function of the numerical parameters introduced in designing the IBE method, namely, the number of surface boundary elements (S), the thickness of each shell h', surrounding the molecular surface, and the cutoff distance H that serves as the outer boundary for the volume integration. As outlined in the previous section, two sets of boundary elements cover the surface. For all of the IBE calculations presented in Table I, the high-density set was placed at a surface-covering density of 4.00 elements/Å^2, which corresponds to 5888 surface elements. These high-density surface elements are grouped into a smaller number S of low-density boundary elements. The first column in Table I gives the number of low-density elements used for each calculation. It is immediately apparent from Table I that Φ_r is approximately 100 times greater than the Φ_{ion}, which arises from the much greater screening effect of the ion charge density by the high dielectric continuum, relative to the solute charge. The agreement between the potentials calculated using the IBE method and the analytical TK solutions is very good; in general, Φ_r is calculated to an accuracy of 1.5% and Φ_{ion} to approximately 15%.

There is relatively little variation in the calculated potentials as a function of the boundary element parameters. Reasonable

(37) Stillinger, F. H., Jr.; Lovett, R. *J. Chem. Phys.* **1968**, *48*, 3858–3868.
(38) Stell, G. *Mod. Theor. Chem.* **1977**, *5*, 47–84.
(39) Kirkwood, J. G. *J. Chem. Phys.* **1934**, *2*, 351–361.
(40) Hill, T. L. *J. Phys. Chem.* **1956**, *60*, 253–255.
(41) Tanford, C.; Kirkwood, J. G. *J. Am. Chem. Soc.* **1957**, *79*, 5333–5339.

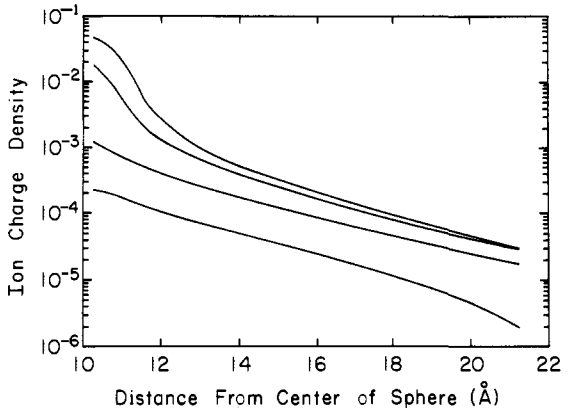

Figure 2. Calculated ion density profile from the NLPB equation along the diameter of the solute sphere, passing through the position of the solute charge. Radius of the sphere = 10 Å, temperature = 300 K, concentration of 1:1 salt = 0.5 M. Starting from the lowest line, the profiles are calculated for d = 0.0, 5.0, 7.5, 8.5 Å, respectively.

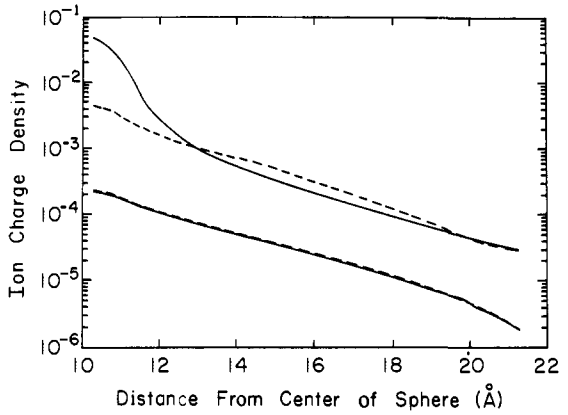

Figure 3. Comparison of the ion density profile, as defined in Figure 2, calculated from the NLPB (full lines) and LPB (dashed lines) equations. The lower pair of lines corresponds to d = 0.0 Å, while the upper pair of lines corresponds to d = 8.5 Å.

values for the various parameters are approximately 200 surface elements, with each h^j = 0.5 Å and a cutoff distance of H = 10.00 Å. For comparison purposes, each of the calculations in Table I was carried out for 10 iterative steps, and the column headed Δ(10) is the value of the integral given in eq 25 after 10 iterative steps. From these results, it is clear that accurate convergence in the ion density is achieved, at least for this example.

Table II presents results for calculations for the 10-Å sphere using the NLPB equation. For this set of calculations, the values of S, h^j, and H are 188, 0.5 Å, and 10.0 Å, respectively (the same as row 2, Table I). We again assume a 1:1 salt and a concentration of 0.5 M; however, unlike Table I, we report calculated potentials for different positions of a unit charge placed along the radius of the sphere. For comparison purposes, we also include in Table II values of Φ_r and Φ_{ion} obtained analytically from the TK treatment of the LPB equation. The last column in Table II is the dimensionless potential ($\Phi e/kT$). It can be seen from this column that, when the solute charge is placed closer to the dielectric boundary than 5 Å, then the linearization condition assumed in deriving the LPB from the full NLPB equation is no longer valid. Figure 2 illustrates the calculated ion charge density along a line directed along the diameter of the sphere and passing through the position of the unit charge. The different lines correspond to the placement of the unit charge at different positions relative to the center of the sphere. If the charge is located at the center of the sphere, then the calculated ion density profile (calculated using the NLPB equation) agrees well with an exponential Debye decay (i.e., the linear Debye–Hückel theory). As the solute charge is moved toward the dielectric boundary, then it can be seen from Figure 2 that the calculated ion density changes

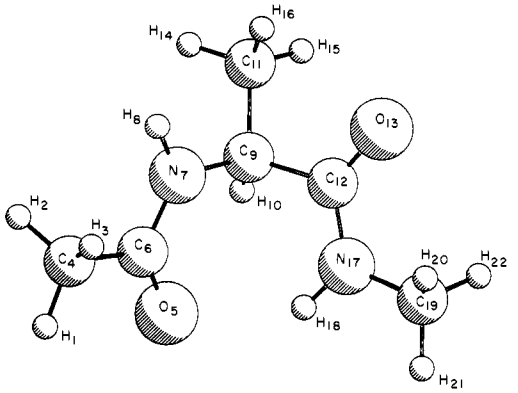

Figure 4. NANMA in C_7^{eq} conformation illustrating the nomenclature used to denote the atoms.

Table III. Illustrative Calculation Using the IBE Method To Solve the NLPB Equation for the NANMA System[a]

Q_m[b]	E_{solv}[c]	E_{ion}[d]	$\lvert\Delta Q_i\rvert$[e]	Δ(10)
0.0	−21.858	0.016	0.027	0.014
+1.0	−127.785	−0.406	0.194	0.015

[a] All energies given in units of kcal mol^{-1}. Total molecular surface area = 164.01 Å^2, H = 10 Å, h^j = 0.5 Å, temp = 300 K, 1:1 salt at 0.5 M. [b] Total molecular charge. [c] $E_{solv} = (1/2)\sum_k q_k \Phi_{r,k}$. [d] $E_{ion} = \sum_k q_k \Phi_{ion,k}$; for a definition of the electrostatic free energy from the NLPB equation, see ref 27. [e] From eq 26.

rapidly near the molecular surface. Figure 3 compares ion density profiles calculated from the LPB equation and the NLPB equation. It can be seen that, when the solute charge is located at the center of the sphere, the agreement between the LPB and NLPB treatments is very good. However, as the solute charge approaches the dielectric boundary, as when d = 8.5 Å, then the ion density profile calculated using the LPB equation is reduced by approximately a factor of 10 (near the surface of the sphere) in comparison to the NLPB equation. Assuming the validity of the NLPB equation for describing the mean field ion distribution, then the apparently incorrect description of the mobile ion distribution by the LPB equation in this region could lead to errors in predicting solvated properties of proteins. This is particularly true in regions where there are protein charges close to each other and exposed to the solvent. In such a case, we expect strong ion binding and formation of ion bridges which will perhaps be better modeled by use of the NLPB equation, rather than by the more diffuse ion densities predicted by the LPB equation.

NANMA. In order to demonstrate that the IBE method can be applied to an arbitrarily-shaped solute molecule, we have calculated solutions of the NLPB equation by assuming a 1:1 salt at 0.5 M for the neutral terminally-blocked amino acid *N*-acetyl-alanyl-*N'*-methylamide (NANMA) and for the fictitious case when this molecule is assumed to possesses an additional unit positive charge, uniformly distributed over the methyl group centered at C_4 (i.e., a third of a unit charged is added to H_1, H_2, H_3), as shown in Figure 4. The charge distribution and atomic radii for neutral NANMA were taken from ref 31. The assumption that NANMA is capable of supporting a unit charge at C_4 is merely for the purpose of demonstrating the utility of the IBE method in obtaining converged solutions of the NLPB equation. The results obtained for this system are summarized in Table III. Figure 5 illustrates convergence in the ionic density, which is achieved after 10 iterations. Not surprisingly, for the calculation on charged NANMA, we observe from our results that the ion density is greatest in the region of the C_4 methyl group, which serves to screen any electrostatic interactions between this methyl group and the rest of the molecule.

Terminally-Blocked Oligo-Lysine. As further illustration of the IBE method, Table IV presents results for terminally-blocked oligo-peptides containing 2 and 10 lysine residues. Each lysine carries a full unit charge. The molecular geometry and charge distribution were obtained using ECEPP/2,[42,43] and the α and

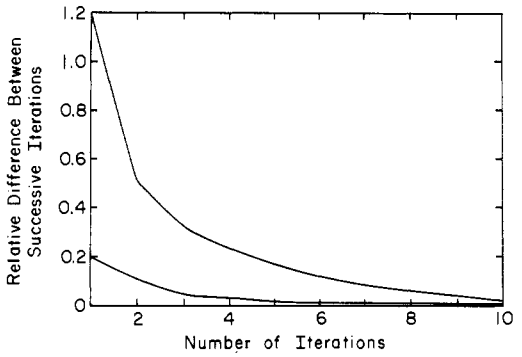

Figure 5. Illustration of the convergence of the IBE method for the NANMA calculation. The lower line corresponds to the neutral system, while the upper line corresponds to the +1 charged system.

Table IV. Illustrative Calculation Using the IBE Method To Solve the NLPB Equation for Terminally Blocked Charged Oligo-Lysines[a]

molecule	total area, Å^2	Q_m[b]	q_{ind}^{comp}	q_{ind}^{ex}	E_{solv}[c]	E_{ion}[d]
di-lysine α-conf	360.3	+2.0	−1.942	−1.974	−183.2	−1.9
di-lysine extend-conf	369.1	+2.0	−1.948	−1.974	−181.4	−1.9
deca-lysine α-conf	1258.3	+10.0	−9.680	−9.873	−2006.1	−32.6

[a] All energies given in units of kcal mol^{-1}. Temperature = 300 K, 1:1 salt at 0.5 M, H = 10 Å, h' = 0.5 Å. [b] Total molecular charge. [c] Defined in footnote *c*, Table III. [d] Defined in footnote *d*, Table III.

extended conformations were chosen. It is well known (see, for example, refs 9 and 21) that application of Gauss' law leads to the following expression for the induced surface charge:

$$q_{ind}^{ex} = Q_m\left[\frac{1}{D_o} - \frac{1}{D_i}\right] \tag{28}$$

where Q_m is the total charge contained within the dielectric boundary (i.e., the molecular charge) and q_{ind}^{ex} is the total induced surface charge given by:

$$q_{ind}^{ex} = \int_S \sigma_r(\mathbf{s})\, d\mathbf{s} \tag{29}$$

Table IV gives the exact value for q_{ind}^{ex} calculated from eq 28 and q_{ind}^{comp}, the value obtained by numerical integration of eq 29 using our computed value of the surface charge density σ_r. It can be seen from Table IV that there is good agreement between q_{ind}^{ex} and q_{ind}^{comp}. The exactness of these calculations is of the same order as those of Zauhar and Morgan.[21]

Discussion

We have presented a new method for obtaining solutions to the NLPB equation, based upon the boundary element method. Although we have found it necessary to introduce a three-dimensional element for the purpose of calculating the ion charge density, this has been done by taking advantage of the boundary element description of the surface, and hence we have an efficient method for carrying out numerical integrations over the region external to the molecular cavity. We have also observed from our calculations that, in regions within 3 Å of the dielectric interface, the NLPB equation predicts a very different ion density compared to the LPB equation.

Although continuum models have been proven useful in recent studies, it is important to recall that they are very simplified models of the liquid state. Their failings are generally well known and are principally connected to the considerable information about the solvent structure that is discarded in assuming a linear dielectric continuum. For example, if the molecular surface possesses a deep concave cavity with exposed polar atoms, then structural features in both the solvent (e.g., water) and free ions (e.g., salt bridges) are expected.[44] It is unlikely that such features can be characterized by the linear dielectric response of bulk water. The use of a spatially isotropic dielectric constant to describe the protein is itself a limitation of the model. Ideally, the dielectric properties of the protein should be connected to the electronic structure of the system. Notwithstanding these limitations, there is a physical underlying basis to continuum models, which probably accounts for their success in predicting solvation free energies and distinguishing between relative hydrated structures of conformationally flexible molecules. The IBE method is itself based upon a very clear physical picture, that of continuity in the dielectric displacement normal to the interface between two regions of different dielectrics. Because of this, it is possible to design an iterative treatment of the IBE method for a large molecule, based upon the decomposition of the molecular surface into fragments. It is possible to couple these fragments together by either exact or approximate descriptions of the dielectric response. We are currently implementing such a method (see Appendix), and estimations suggest that the division of the surface into fragments of the order of hundreds of Å^2 will lead to significant acceleration in the calculation of the total electrostatic potential around a macromolecule.

In summary, we have described a method for computing the total electrostatic potential obtained from the NLPB equation, based upon the boundary element method. The method makes use of the advantageous features of boundary element techniques to solve the Poisson equation, such as the accurate description of the molecular surface, and makes use of the boundary element description of the molecular surface in the design of an efficient procedure to evaluate integrals numerically over the volume external to the molecular cavity. We have demonstrated that the IBE method for obtaining approximate numerical solutions to the NLPB equation can be used to reproduce analytical Tanford–Kirkwood solutions for model spherical systems at ionic strengths ≤1 M. The calculation on terminally-blocked alanine and the two oligo-lysine peptides demonstrates that the procedure is sufficiently general to admit arbitrary cavity shapes in the description of the solute.

Appendix

Number of Operations Required by the IBE and FD Methods. In the following, we estimate the ratio η_P between the number of operations required to solve the Poisson equation using the IBE method and the FD method. The corresponding ratio η_{NLPB} for the NLPB equation is also estimated.

The number of operations required by the IBE method has already been given in eq 21. However, for a large molecule such as a protein, it is possible to modify the procedure by partitioning the molecular surface into a number of pieces. The molecular surface S is now the union of N_p surface pieces. The integral eq 5 can accordingly be transformed into N_p coupled matrix equations; thus:

$$\mathbf{K}_p\sigma_p = \mathbf{b} - \sum_{l\neq p}^{N_p} \mathbf{K}_l\sigma_l \tag{A1}$$

where $p = 1, ..., N_p$, $\mathbf{K}_p$ is the matrix appearing in eq 13 defined in terms of those boundary elements belonging to piece p; σ_p is the surface charge density on piece p, $\mathbf{b}$ is the normal component of the electrostatic field due to the molecular charge distribution, and the last term gives the electrostatic field of surface charge density σ_l on all of the other surface pieces. The coupled set of equations in (A1) can be solved iteratively to obtain the surface charge density on each fragment of the molecular surface; thus:

$$\sigma_p^t = \mathbf{K}_p^{-1}(\mathbf{b} - \sum_{l\neq p}^{N_p} \mathbf{K}_l\sigma_l^{(t-1)}) \tag{A2}$$

where t is the iteration number. We find the iterative solution

(42) Nemēthy, G.; Pottle, M. S.; Scheraga, H. A. *J. Phys. Chem.* **1983**, *87*, 1883–1887.
(43) Sippl, M. J.; Nemēthy, G.; Scheraga, H. A. *J. Phys. Chem.* **1984**, *88*, 6231–6233.
(44) Ben-Naim, A.; Ting, K. L.; Jernigan, R. L. *Biopolymers* **1990**, *29*, 901–919.

of eq A2 to an accuracy of approximately 10^{-4} to be sufficiently fast, with convergence after n_{it}^{p} iterations, where $n_{it}^{p} \leq 20$ for the calculations that we have considered so far. It follows that the number of operations to solve equations (A1) and (A2) iteratively is

$$n_{BE}^{p} = N_p\left(\frac{S}{N_p}\right)^3 + \left(\frac{S}{N_p}\right)^2 N_p^2 n_{it}^{p} \tag{A3}$$

We have found that assignment of the surface elements to the nearest surface atom provides the optimal partitioning of the molecular surface. In this case, the number of pieces N_p given by

$$N_p = S/\langle s_p \rangle \tag{A4}$$

where $\langle s_p \rangle$ is the average surface area per exposed atom. Substitution of eq A4 into eq A3 shows that the first term in eq A3 is first order in S, while the second term is second order in S. For big molecules with a large molecular surface, the number of operations required to find a sufficiently accurate approximate solution of eq 13 is dominated by the second term in eq A3; thus:

$$n_{BE}^{p} \approx S^2 n_{it}^{p} \tag{A5}$$

while straightforward solution of eq 13 requires $\approx S^3$ operations. Recently, Nicholls and Honig[18] have presented a very elegant accelerated FD algorithm utilizing the successive over-relaxation method. The FD method transforms the LPB equation into the matrix equation

$$\Phi = \mathbf{F}\Phi + \mathbf{d} \tag{A6}$$

where Φ is an N^3-dimensional vector of the values of the potential in cells of rectangular grid and F is a matrix of six diagonals. The algorithm of Nicholls and Honig requires n_{FD}^{a} operations to solve the NLPB equation, where

$$n_{FD}^{a} = N^4 n_d n_{it}^{ex} \tag{A7}$$

where n_d is the number of matrix diagonals, n_{it}^{ex} is the number of iterations to distribute *excess* ion charge. To obtain a solution of the NLPB equation, it is necessary to make $n_{it}^{ex} = 10$–20 iterations of the LPB equation. However, it should be noted that it is not necessary to come to complete convergence at each iteration of the LPB equation.[45] Therefore, an effective value of n_{it}^{ex} is ≈ 2–4. Hence a final estimation of the ratio between the number of operations required by the IBE and FD methods is given by:

$$\eta = \frac{S^2 n_{it}^{p}}{n_d N^4} + \frac{n_{sh}^2 n_{it}^{b} S^2}{n_d n_{it}^{ex} N^4} \tag{A8}$$

where the first term is the ratio η_P, while the second term is the ratio η_{NLPB}. Expression A8 demonstrates that the IBE method requires the same order of operations as the FD method so long as $S \approx N^2$ and values of n_d, n_{it}^{ex}, n_{it}^{b}, n_{sh} are independent of N, S and are of the order 10–20. To obtain numerical estimations of η_P and η_{NLPB}, consider the example of a spherical molecule having radius $R = 15$ Å, and a thickness of the ion atmosphere $H = 10$ Å. Since reasonable area of each surface element is 1 Å^2, the value of S is ≈ 3000, the corresponding length of the lattice side for the FD method should be L ≈ 50 Å, and the size of rectangular cells should be about $h^j = 0.5$ Å or $N = 100$. Hence, we find that at approximately the same level of accuracy, $\eta_P = 0.1$ and $\eta_{NLPB} = 10$. In addition, we obtained the following CPU times for the IBE method running on a single processor of an IBM ES/3090 for the di-lysine calculation. For this calculation, solution of eq A1 and evaluation of the solvation free energy requires 23 s (seconds), one iteration of the NLPB requires 17 s, and the total time for the solution of the NLPB equation, including evaluation of the energy of interaction of the solute with the mobile ions, requires 151 s. In the case of deca-lysine, these times are equal to 219 s, 191 s, and 1250 s, respectively. We are still developing much of the code used for these calculations and hope to improve the performance. The main purpose of this Appendix has been to present an outline of the inherent complexity of the IBE method and tentatively to suggest its optimal performance. The IBE method requires a smaller number of operations to solve the Poisson equation, but the algorithm by Nicholls and Honig will generally be faster than the IBE method to solve the NLPB equation. The IBE method for solving the NLPB equation does, however, incorporate some of the advantageous features of the boundary element method, principally an accurate description of the dielectric boundary; it also permits the use of generalized descriptions of the solute charge distribution, and gives rise to a flexible and accurate volume integration to obtain the ion density.

Acknowledgment. We acknowledge the very important work of R. L. Williams in developing much of the boundary element code used for some of the calculations in this paper, and J. P. Bond for useful and stimulating discussions. We also thank A. Nicholls for helpful comments on the work of ref 18. This work was supported by Grant No. GM-14312 from the National Institute of General Medical Sciences of the National Institutes of Health, and by Grant Nos. DMB84-01811 and DMB90-15815 from the National Science Foundation. Support was also received from the National Foundation for Cancer Research. The computations were carried out at the Cornell National Supercomputer Facility, a resource of the Cornell Center for Theory and Simulation in Science and Engineering, which receives major funding from the National Science Foundation and IBM corporation, with additional support from New York State and members of its Corporate Research Institute.

(45) Nicholls, A. Private communication.